Nonlinear Dyn (2019) 97:2595–2605
https://doi.org/10.1007/s11071-019-05150-y

ORIGINAL PAPER

Position tracking control for permanent magnet linear motor via fast nonsingular terminal sliding mode control

Jin Li · Haibo Du · Yingying Cheng · Guanghui Wen · Xiuping Chen · Canghua Jiang

Received: 27 December 2018 / Accepted: 16 July 2019 / Published online: 30 July 2019

Abstract In this paper, for the position control problem of permanent magnet linear motors, a fast nonsingular terminal sliding mode control (FNTSMC) method based on the finite-time disturbance observer (FTDO) is proposed. By employing a fast nonsingular terminal sliding surface, the FNTSMC is designed. Besides, a FTDO is applied to estimate the disturbance and the estimation is served as compensation for the controller. A rigorous analysis based on the Lyapunov stability theory is provided to prove that the proposed control method can achieve faster dynamic response characteristic and higher steady accuracy than the linear sliding mode control method and the PID control method. Numerical simulation results are explored to illustrate the superiority of the proposed approach.

Keywords Fast nonsingular terminal sliding mode control · Finite-time disturbance observer · Permanent magnet linear motor · Robustness

J. Li · H. Du (✉) · Y. Cheng · X. Chen · C. Jiang
School of Electrical Engineering and Automation, Hefei University of Technology, Hefei 230009, Anhui, People's Republic of China
e-mail: haibo.du@hfut.edu.cn

G. Wen
School of Mathematics, Southeast University, Nanjing 210096, Jiangsu, People's Republic of China

G. Wen
School of Engineering, RMIT University, Melbourne, VIC 3001, Australia

1 Introduction

Nowadays, the permanent magnet linear motor (PMLM) is playing an increasingly important role in civil, industrial and military applications [1,2].In particular, it is broadly implemented in the precision manufacturing industries as a result of its high thrust density, high acceleration, high speed, high precision. Consequently, the research of PMLM is recently getting more conspicuous attentions by the research community. The principal limitations confronted by a PMLM are the external disturbances, force ripples and frictions [3]. From the perspective of motion control, it is crucial to achieve the fast dynamic response and improve the tracking precision property of PMLM.

There are numerous control algorithms already applied for analysis and design of PMLM in the recent literature. In [4], a robust adaptive algorithm was presented for offset of friction and force ripple generated by PMLM. A water-cooled PMLM system was modeled, and its temperature characteristics were investigated under various working duties in [5]. The closed-loop speed control performance of PMLM based on primary flux-oriented control was studied in [6]. The sliding mode control (SMC), which is a preferred method to handle the control problems of nonlinear systems, has been resoundingly used in the practical project since it is insensitive to parameter change and interference in [7–13]. In [14], an adaptive 2-SMC method is proposed for a class of unknown multi-input multi-output nonlinear discrete systems. In [15], combining the SMC and data-driven control method, the stable pressure control was solved for the gas collectors of coke ovens. Nevertheless, the traditional SMC only ensures the asymptotic stability of the closed-loop system in the sliding mode phase while the system states converge to the equilibrium point at an infinite time.

Due to the superiority of finite-time convergence [16–18], the terminal sliding mode control (TSMC) was presented in [19–22]. Moreover, the nonsingular TSMC (NTSMC) was proposed to avert the singularity and applied in some practical control systems [23–26]. Even so, the internal discontinuity occurs the aforementioned TSMC schemes as ever. Accordingly, there are some efficient techniques that have been used to overcome the chattering problem as a result of the internal discontinuity, such as full-order SMC [27] and the fast nonsingular terminal sliding mode control (FNTSMC) [28–35]. Specifically, the FNTSMC can obtain a fast state convergence to improve tracking accuracy as well as restrain the chattering problem. In this paper, inspired by these merits of the FNTSMC method, we apply the FNTSMC method to a PMLM system.

However, the FNTSMC-based PMLM system copes with the uncertainties by making a trade-off between control performance and robustness. One effective approach, which can not only guarantee the control performance but also improve the robustness, is feedforward compensation of the disturbances [36–38]. The observer-design approach is effective to estimate the disturbances, such as sliding mode observer [39,40] and finite-time observer [41,42]. Motivated by the finite-time observer, a novel finite-time disturbance observer (FTDO) is adopted in this paper to provide the estimation of the lumped disturbances and implement the feedforward compensation.

The major contributions of this paper are: (1) A fast nonsingular terminal sliding mode surface is designed to achieve the fixed-time stability, i.e., the system state will converge to the equilibrium in a fixed time independent of initial condition, which overcomes the shortcoming that the TSMC has a slower convergence rate than the linear sliding mode controller (LSMC) when the system state is far away from the equilibrium. Additionally, a FNTSMC algorithm with good performance in robustness and chattering reduction is proposed to realize the highly accurate position tracking control for a PMLM system. (2) A higher-order FTDO is applied to estimate the time-varying disturbances, and then, the estimated values are used as feedforward compensation of the disturbances. (3) A theoretical stability analysis of the closed-loop system and corresponding simulation results are provided to show the effectiveness of the proposed control algorithm. In addition, it is clearly seen the superiority of the proposed method in comparison with some existing ones.

The remainder of this paper is organized as follows. In Sect. 2, the PMLM system model and control objective are introduced. In Sect. 3, A FNTSMC controller with the finite-time disturbance observer is proposed and its stability is analyzed. Simulations results are implemented to demonstrate the effectiveness of the proposed control strategy in Sect. 4. The conclusions of this paper are given in Sect. 5.

2 System description and problem formulation

2.1 Model of PMLM

The mathematical model of PMLM can be expressed as follows [43]:

$$\begin{aligned} \dot{p}_1(t) &= p_2(t), \\ \dot{p}_2(t) &= -\frac{L_f L_e}{Rm} p_2(t) + \frac{L_f}{Rm} u(t) - \frac{d(t)}{m}, \\ y(t) &= p_1(t), \end{aligned} \tag{1}$$

where p_1 denotes the position, the velocity is denoted by p_2 , $u(t)$ represents the control input, R denotes the resistance, m denotes the motor mass, L_f and L_e denote the force constant and the back electromotive force, respectively. The lumped disturbance named $d(t)$ is composed of friction force, ripple force and external disturbance, etc.

2.2 Control objective

The PMLM control system is designed to ensure that the reference trajectory can be tracked by the actual motor's position. Let $p_r(t)$ denote the reference linear displacement, whose first-order and second-order derivatives are assumed to be bounded.

For simplicity, denote

$$a = \frac{L_f L_e}{Rm}, \quad b = \frac{L_f}{Rm}, \quad F = -\frac{d(t)}{m}, \tag{2}$$

then Eq. (1) can be rewritten as follows:

$$\begin{aligned} \dot{p}_1(t) &= p_2(t), \\ \dot{p}_2(t) &= -ap_2(t) + bu(t) + F, \\ y(t) &= p_1(t). \end{aligned} \tag{3}$$

The main objective of this paper is to design a controller for PMLM such that the position signal $y = p_1$ can track the reference signal p_r. To improve the dynamical performance and disturbance rejection performance, the method of fast nonsingular terminal sliding mode control (FNTSMC) will be employed. For the convenience of controller design and stability analysis, the error dynamical system is derived.

Define

$$\begin{aligned} e_1(t) &= p_r(t) - p_1(t), \\ e_2(t) &= \dot{p}_r(t) - p_2(t), \end{aligned} \tag{4}$$

as the tracking errors for linear displacement and speed signal. Then we can obtain the following error dynamic equation from (3) :

$$\begin{aligned} \dot{e}_1(t) &= e_2(t), \\ \dot{e}_2(t) &= -ae_2(t) - bu - F + a\dot{p}_r + \ddot{p}_r, \\ y &= p_1. \end{aligned} \tag{5}$$

About the disturbance, the following assumption is made in this paper.

Assumption 1 For PMLM system (3), the lumped disturbance F is assumed to satisfy that

(1) $|F| \le d^*$ with a constant d^*,
(2) the $n - 1$ time derivatives of F is existing and $|F^{(n-1)}| \le \varsigma$, where ς is a positive constant.

2.3 Some definitions and lemmas

Definition 1 (*Finite-time stability*) [44] Consider the system

$$\dot{x} = f(x), \quad f(0) = 0, x(0) = x_0, \quad x \in R^n, \tag{6}$$

where $f(\cdot) : R^n \to R^n$ is continuous. The equilibrium $x = 0$ of system (6) is finite-time stable if it is Lyapunov stable and finite-time convergent, i.e., there exists a finite time $T(x_0)$ which is dependent on the initial condition x_0 such that $\lim_{t\to T(x_0)} x(t) = 0$ and $x(t) = 0$ for all $t \ge T(x_0)$.

Definition 2 Denote $\text{sig}^\alpha(x) = \text{sign}(x)|x|^\alpha$, where $\alpha > 0, x \in \mathcal{R}$, $\text{sign}(\cdot)$ is the standard sign function.

Lemma 1 [44] *For the system (6), suppose that there exists a positive definite and proper function $V(x) : R^n \to R$ such that $\frac{\partial V(x)}{\partial x} f(x) + c(V(x))^\alpha \le 0$ for all $x \in R^n$, where $c > 0$, $\alpha \in (0, 1)$. Then, this system is globally finite-time stable.*

Lemma 2 [45] *For the system (6), suppose that there exists a continuous, positive definite function $V(x) : R^n \to R$ such that $\dot{V}(x) \le -\alpha V^p(x) - \beta V^q(x)$, where $\alpha > 0, \beta > 0, 0 < p < 1, q > 1$. Then the origin is a fixed-time stable equilibrium and the fixed convergent time satisfies $T \le \frac{1}{\alpha(1-p)} + \frac{1}{\beta(q-1)}$.*

Lemma 3 [46] *For any $x_1, x_2 \in R$ and a real number $p \in (0, 1]$, $(|x_1| + |x_2|)^p \ge 2^{(p-1)}(|x_1|^p + |x_2|^p)$.*

Lemma 4 [47] *The inequality*

$$|x|^c|y|^d \le \frac{c}{c+d}\gamma|x|^{c+d} + \frac{d}{c+d}\gamma^{-c/d}|y|^{c+d}$$

holds $\forall x, y \in \mathcal{R}$, and $\forall c, d, \gamma > 0$.

3 Finite-time disturbance observer-based FNTSMC control method

3.1 Design of a finite-time disturbance observer

To handle the time-varying disturbance $F(t)$, a finite-time disturbance observer is employed to estimate the disturbance.

Theorem 1 *For PMLM system (3) under Assumption 1, if the disturbance observer is chosen as*

$$\begin{aligned} \dot{\hat{q}}_1 &= -ap_2 + bu + \hat{q}_2 + f_1\text{sig}^{r_1}(p_2 - \hat{q}_1), \\ \dot{\hat{q}}_2 &= \hat{q}_3 + f_2\text{sig}^{r_2}(p_2 - \hat{q}_1), \\ &\vdots \\ \dot{\hat{q}}_{n-1} &= \hat{q}_n + f_{n-1}\text{sig}^{r_{n-1}}(p_2 - \hat{q}_1), \\ \dot{\hat{q}}_n &= f_n\text{sig}^{r_n}(p_2 - \hat{q}_1), \\ \hat{F} &= \hat{q}_2 \end{aligned} \tag{7}$$

then

(1) *if the disturbance is constant, the disturbance estimation $\hat{F}$ will converge to the real disturbance F in a finite time,*

(2) *if the disturbance is time varying, the disturbance estimation error will converge to a bounded region in a finite time, i.e.,* $|\hat{F} - F| \le \sigma$ *with a constant* σ,

where $f_i > 0$ *are appropriate positive gains,* $r_i = 1 + i\tau, \tau \in (-\frac{1}{n}, 0), (i = 1, 2, \ldots, n)$.

Proof We will analyze the stability of the proposed observer based on Lyapunov method.

Suppose that the estimation errors are defined as

$$\begin{aligned} w_1 &= p_2 - \hat{q}_1, \\ w_2 &= F - \hat{q}_2, \\ w_3 &= \dot{F} - \hat{q}_3, \\ &\vdots \\ w_n &= F^{(n-2)} - \hat{q}_n, \end{aligned} \tag{8}$$

then the estimation error dynamics of the FTDO (7) are given by:

$$\begin{cases} \dot{w}_1 = w_2 - f_1 \mathrm{sig}^{r_1}(w_1) \\ \dot{w}_2 = w_3 - f_2 \mathrm{sig}^{r_2}(w_1) \\ \dot{w}_3 = w_4 - f_3 \mathrm{sig}^{r_3}(w_1) \\ \ldots \\ \dot{w}_{n-1} = w_n - f_{n-1} \mathrm{sig}^{r_{n-1}}(w_1) \\ \dot{w}_n = F^{(n-1)} - f_n \mathrm{sig}^{r_n}(w_1). \end{cases} \tag{9}$$

For the error system (9) when $F^{(n-1)} = 0$, it follows from [41] that there is a positive and radially unbounded Lyapunov function $V(w)$ such that

$$\dot{V}(w) \le -cV^{\alpha}(w) \tag{10}$$

where $c > 0, \alpha \in (0, 1)$. If $F^{(n-1)} \ne 0$ and $|F^{(n-1)}| \le \varsigma$, then

$$\dot{V}(w) \le -cV^{\alpha}(w) + \left|\frac{\partial V(w)}{\partial w_n}\right|\varsigma \tag{11}$$

By [41] and the homogeneous system theory, it can be concluded that there is a positive constant $\hat{c} > 0$ and a fractional power $\beta \in (0, \alpha)$ such that

$$\left|\frac{\partial V(w)}{\partial w_n}\right| \le \hat{c}V^{\beta}(w). \tag{12}$$

It follows from Lemma 4 that there is a constant $M > 0$ such that

$$\left|\frac{\partial V(w)}{\partial w_n}\right|\varsigma \le \frac{c}{2}V^{\alpha}(w) + M, \tag{13}$$

which leads to

$$\dot{V}(w) \le -\frac{c}{2}V^{\alpha}(w) + M. \tag{14}$$

As a result, there exits a time $T_{\mathrm{f}} \in R^+$, for $\forall t > T_{\mathrm{f}}, |w_i| \le \delta_i, (i = 1, 2, \ldots, n)$ with δ_i being positive constants, which means that the estimation errors converge to a bounded region in a finite time. □

Remark 1 Although the main proofs for Theorem 1 are motivated by the work [41], the difference is that here the higher-order finite-time observer is used to estimate the external disturbance while the work [41] just consider the observer design for time-varying nonlinear systems satisfying certain assumptions.

3.2 Design of fast nonsingular terminal sliding mode controller

Based on the previous disturbance observer, this section will design a fast nonsingular terminal sliding mode controller.

Step 1: design of a fast nonsingular terminal sliding mode surface

Different from the conventional nonsingular terminal sliding mode surface, a fast nonsingular terminal sliding mode surface is chosen as:

$$s = e_1 + \beta_2 \mathrm{sig}^{\gamma_2}(e_1) + \beta_1 \mathrm{sig}^{\gamma_1}(e_2) \tag{15}$$

with $\beta_1 > 0$, $1 < \gamma_1 < 2$, $\beta_2 > 0$, $\gamma_1 < \gamma_2$.

If the sliding mode surface $s = 0$ can be reached in a finite time, then one obtains that

$$e_1 + \beta_2 \mathrm{sig}^{\gamma_2}(e_1) + \beta_1 \mathrm{sig}^{\gamma_1}(e_2) = 0. \tag{16}$$

Choose Lyapunov function $W = \frac{1}{2}e_1^2$, whose derivative is

$$\dot{W} = e_1\dot{e}_1 = e_1 e_2. \tag{17}$$

Meanwhile, it follows from (16) that

$$e_2 = -\beta_1^{-\frac{1}{\gamma_1}} \mathrm{sig}^{\frac{1}{\gamma_1}}(e_1 + \beta_2 \mathrm{sig}^{\gamma_2}(e_1))$$
$$= -\beta_1^{-\frac{1}{\gamma_1}} \mathrm{sign}(e_1 + \beta_2 \mathrm{sig}^{\gamma_2}(e_1)) \times |e_1 + \beta_2 \mathrm{sig}^{\gamma_2}(e_1)|^{\frac{1}{\gamma_1}}$$
$$= -\beta_1^{-\frac{1}{\gamma_1}} \mathrm{sign}(e_1) \times (|e_1| + \beta_2 |e_1|^{\gamma_2})^{\frac{1}{\gamma_1}}. \tag{18}$$

Based on Lemma 4, substituting the equality (18) into (17) results in

$$\dot{W} \le -\beta_1^{-\frac{1}{\gamma_1}} |e_1| (|e_1| + \beta_2 |e_1|^{\gamma_2})^{\frac{1}{\gamma_1}}$$
$$\le -2^{\frac{1-\gamma_1}{\gamma_1}} \beta_1^{-\frac{1}{\gamma_1}} |e_1|^{\frac{1}{\gamma_1}+1} - 2^{\frac{1-\gamma_1}{\gamma_1}} \left(\frac{\beta_2}{\beta_1}\right)^{\frac{1}{\gamma_1}} |e_1|^{\frac{\gamma_2}{\gamma_1}+1}. \tag{19}$$

Based on the definition of W, it can be obtained that

$$\dot{W} \le -2^{\frac{3-\gamma_1}{2\gamma_1}} \beta_1^{-\frac{1}{\gamma_1}} W^{\frac{\gamma_1+1}{2\gamma_1}} - 2^{\frac{2-\gamma_1+\gamma_2}{2\gamma_1}} \left(\frac{\beta_2}{\beta_1}\right)^{\frac{1}{\gamma_1}} W^{\frac{\gamma_1+\gamma_2}{2\gamma_1}}. \tag{20}$$

According to the range of gains (15), we can know that $\frac{3}{4} \le \frac{\gamma_1+1}{2\gamma_1} \le 1$, $\frac{\gamma_1+\gamma_2}{2\gamma_1} > 1$. Then, based on the Lemma 2, it can be concluded that the error e_1 will reach zero in a fixed time.

Step 2: design of a fast nonsingular terminal sliding mode control law

In this step, we will design a fast nonsingular terminal sliding mode controller such that the sliding mode surface $s = 0$ can be reached as close as possible.

Theorem 2 *For the error dynamic system (5), if the nonsingular terminal sliding mode controller is designed as*

$$u = u_1 + u_2,$$
$$u_1 = \frac{1}{b}\Big(- ae_2 + a\dot{p}_r + \ddot{p}_r - \hat{F} + \frac{1}{\beta_1\gamma_1} \mathrm{sig}^{2-\gamma_1}(e_2) + \frac{\beta_2\gamma_2}{\beta_1\gamma_1} \mathrm{sig}^{2-\gamma_1}(e_2)|e_1|^{\gamma_2-1}\Big),$$
$$u_2 = \frac{1}{b}\Big(k_1 s + k_2 \mathrm{sig}^{\gamma_3}(s)\Big),$$
$$s = e_1 + \beta_2 \mathrm{sig}^{\gamma_2}(e_1) + \beta_1 \mathrm{sig}^{\gamma_1}(e_2), \tag{21}$$

where $k_1 > 0$, $k_2 > d^*$, $\beta_1 > 0$, $\beta_2 > 0$, $0 < \gamma_3 < 1$, then

- *(1) the sliding variable s will converge to the following region in a fixed time:*

$$|s| \le \Phi = min(\Phi_1, \Phi_2) \tag{22}$$

where

$$\Phi_1 = \frac{\sigma}{k_1}, \Phi_2 = \left(\frac{\sigma}{k_2}\right)^{\frac{1}{\gamma_3}}. \tag{23}$$

- *(2) the tracking error e_1 and its derivative e_2 will converge to the following region in a fixed time:*

$$|e_1| \le \left(\frac{\Phi}{\beta_2}\right)^{\frac{1}{\gamma_2}}, |e_2| \le \left(\frac{\Phi}{\beta_1}\right)^{\frac{1}{\gamma_1}}. \tag{24}$$

Proof We first analyze the boundedness before the observer converges to the ultimate steady-state region. Denote $\lambda_1 = F - \hat{F}$. Choose the following Lyapunov function

$$V = \frac{1}{2}s^2 + \frac{1}{2}\lambda_1^2$$
$$= V_1 + V_2. \tag{25}$$

Based on (25), the corresponding derivative is

$$\dot{V} = \dot{V}_1 + \dot{V}_2$$
$$= s\dot{s} + \lambda_1\dot{\lambda}_1$$
$$= s(e_2 + \beta_1\gamma_1|e_2|^{\gamma_1-1}\dot{e}_2 + \beta_2\gamma_2|e_1|^{\gamma_2-1}\dot{e}_1) + \lambda_1\dot{\lambda}_1. \tag{26}$$

It follows from (26) that

$$\dot{V} = s\Big(e_2 + \beta_1\gamma_1|e_2|^{\gamma_1-1}(-ae_2 - bu + F + a\dot{p}_r + \ddot{p}_r) + \beta_2\gamma_2|e_1|^{\gamma_2-1}\dot{e}_1\Big) + \lambda_1\dot{\lambda}_1 \tag{27}$$

Substituting (21) into (27) leads to

$$\dot{V} = s\Big[e_2 + \beta_1\gamma_1|e_2|^{\gamma_1-1}\Big(- ae_2 - b(u_1+u_2) + F + a\dot{p}_r + \ddot{p}_r\Big) + \beta_2\gamma_2|e_1|^{\gamma_2-1}\dot{e}_1\Big] + \lambda_1\dot{\lambda}_1$$
$$= s\Big[- \beta_1\gamma_1|e_2|^{\gamma_1-1}\Big(k_1 s + k_2\mathrm{sig}^{\gamma_3}(s) - \lambda_1\Big)\Big] + \lambda_1\dot{\lambda}_1$$

$$= -\beta_1\gamma_1|e_2|^{\gamma_1-1}\left(k_1s^2+k_2|s|^{1+\gamma_3}-\lambda_1 s\right)+\lambda_1\dot{\lambda}_1. \tag{28}$$

From the disturbance observer proposed in Theorem 1, it can be found that the state $(\lambda_1, \dot{\lambda}_1)$ is always bounded. Assume that there are two constants L_1, L_2 such that

$$|\lambda_1| \le L_1, \quad |\dot{\lambda}_1| \le L_2. \tag{29}$$

Under this assumption, it follows from (28) that

$$\begin{aligned}\dot{V} \le&\beta_1\gamma_1|e_2|^{\gamma_1-1}\left(-k_1s^2-k_2|s|^{1+\gamma_3}+L_1|s|\right)+L_1L_2\\ =&\beta_1\gamma_1|e_2|^{\gamma_1-1}\left(-k_1(|s|-L_1)|s|-k_2|s|^{1+\gamma_3}\right)+L_1L_2.\end{aligned} \tag{30}$$

Clearly, if the state $|s| \ge L_1$, then it follows from (30) that

$$\dot{V} \le L_1L_2, \tag{31}$$

which implies that the function V (and then the state s) will be bounded during the time interval $[0, T^*]$.

After the time T^*, when the disturbance observer error λ_1 converges to the region Φ, it follows from (28) that

$$\begin{aligned}\dot{V}_1 =& s\dot{s}\\ =& -\beta_1\gamma_1|e_2|^{\gamma_1-1}\left(k_1s^2+k_2|s|^{1+\gamma_3}-\lambda_1 s\right)\\ \le& -\beta_1\gamma_1|e_2|^{\gamma_1-1}\left(k_1s^2+k_2|s|^{1+\gamma_3}-\sigma|s|\right).\end{aligned} \tag{32}$$

Next, we will analyze the relation (32) in two cases.

Case 1 Rewrite (32) as the following form:

$$\dot{V}_1 \le -\beta_1\gamma_1|e_2|^{\gamma_1-1}\left(\left(k_1-\frac{\sigma}{|s|}\right)s^2+k_2|s|^{1+\gamma_3}\right). \tag{33}$$

If $|s| > \sigma/k_1$ and $e_2 \ne 0$, there are two positive constants c_1, c_2 such that

$$\dot{V}_1 \le -c_1s^2-c_2|s|^{\gamma_3+1} = -2c_1V_1-2^{\frac{\gamma_3+1}{2}}c_2V_1^{\frac{\gamma_3+1}{2}} \tag{34}$$

Therefore, the finite-time stability can be guaranteed according to Lemma 1. In other words, the system state will converge to the following region in a fixed time:

$$|s| \le \frac{\sigma}{k_1} \tag{35}$$

Case 2 Rewrite (32) as the following form:

$$\dot{V}_1 \le -\beta_1\gamma_1|e_2|^{\gamma_1-1}\left(k_1s^2+\left(k_2-\frac{\sigma}{|s|^{\gamma_3}}\right)|s|^{1+\gamma_3}\right). \tag{36}$$

If $|s| > (\frac{\sigma}{k_2})^{\frac{1}{\gamma_3}}$ and $e_2 \ne 0$, there are two positive constants c_3, c_4 such that

$$\dot{V}_1 \le -c_3s^2-c_4|s|^{\gamma_3+1} = -2c_3V_1-2^{\frac{\gamma_3+1}{2}}c_4V_1^{\frac{\gamma_3+1}{2}} \tag{37}$$

Similar to the case 1, the system state will converge to the following region in a fixed time:

$$|s| \le \left(\frac{\sigma}{k_2}\right)^{\frac{1}{\gamma_3}} \tag{38}$$

The last step is to illustrate that $e_2 = 0$ for the aforesaid two cases is not an attractor in the reaching stage. Using (21) into (5) for $e_2 = 0$, we obtain

$$\begin{aligned}\dot{e}_2 &= -k_1s-k_2\mathrm{sig}^{\gamma_3}(s)-\hat{F}+F\\ &= -k_1s-k_2\mathrm{sig}^{\gamma_3}(s)+\lambda_1\end{aligned} \tag{39}$$

i.e.,

$$\dot{e}_2 = \begin{cases}-\left(k_1-\frac{\lambda_1}{s}\right)s-k_2\mathrm{sig}^{\gamma_3}(s) \ne 0, \text{for}|s| > \Phi_1\\ -k_1s-\left[k_2-\frac{\lambda_1}{\mathrm{sig}^{\gamma_3}(s)}\right]\mathrm{sig}^{\gamma_3}(s) \ne 0, \text{for}|s| > \Phi_2\end{cases} \tag{40}$$

It means that the fixed-time reachability of s can also be guaranteed if $e_2 = 0$.

We can conclude from (35) and (38) that the sliding variable s reaches the region $|s| \le \Phi = \min(\Phi_1, \Phi_2)$ in a fixed time.

Next, we prove the convergence of the tracking error and its first derivative in (24). Equation (15) can be rewritten as:

$$e_1+\left[\beta_1-\frac{s}{\mathrm{sig}^{\gamma_1}(e_2)}\right]\mathrm{sig}^{\gamma_1}(e_2)+\beta_2\mathrm{sig}^{\gamma_2}(e_1) = 0 \tag{41}$$

Then if $\beta_1 - \frac{s}{\mathrm{sig}^{\gamma_1}(e_2)} > 0$, Eq. (41) is kept in the same form of FNTSMC as that of (15), which also demonstrate that the velocity error will converge to the following region in a fixed time:

$$|e_2| \leq \left(\frac{\Phi}{\beta_1}\right)^{\frac{1}{\gamma_1}} \tag{42}$$

Homoplastically, Eq. (15) can also be rewritten as:

$$e_1 + \beta_1 \mathrm{sig}^{\gamma_1}(e_2) + \left[\beta_2 - \frac{s}{\mathrm{sig}^{\gamma_2}(e_1)}\right] \mathrm{sig}^{\gamma_2}(e_1) = 0 \tag{43}$$

Using a same analysis as that in (41), if $\beta_2 - \frac{s}{\mathrm{sig}^{\gamma_2}(e_1)} > 0$, it follows from (22) that the tracking error will converge to the following region in a fixed time:

$$|e_1| \leq \left(\frac{\Phi}{\beta_2}\right)^{\frac{1}{\gamma_2}} \tag{44}$$

□

Remark 2 Note that there is no singularity for the proposed control law (21) with the conditions $1 < \gamma_1 < 2$ and $\gamma_2 > \gamma_1$ as that the nonsingular terminal sliding mode control law in [23].

Remark 3 Once all fractional powers in (21) are set to 1 (i.e., $\gamma_1 = \gamma_2 = \gamma_3 = 1$), the control method is reduced to the linear sliding mode control (LSMC) which has the following form:

$$\begin{aligned} u &= u_1 + u_2, \\ u_1 &= \frac{1}{b}\Big(-ae_2 + a\dot{p}_r + \ddot{p}_r + \hat{F} + \frac{1}{\beta_1\gamma_1}e_2 + \frac{\beta_2\gamma_2}{\beta_1\gamma_1}e_2\Big), \\ u_2 &= \frac{1}{b}\Big(k_1 s + k_2 s\Big), \\ s &= e_1 + \beta_2 e_1 + \beta_1 e_2. \end{aligned} \tag{45}$$

In simulation, it will be shown that the proposed method has a faster dynamic performance and better robustness than the linear sliding mode control method.

The control block diagram of PMLM is shown in Fig. 1, and next we will verify the effectiveness of the proposed algorithm via the simulation results.

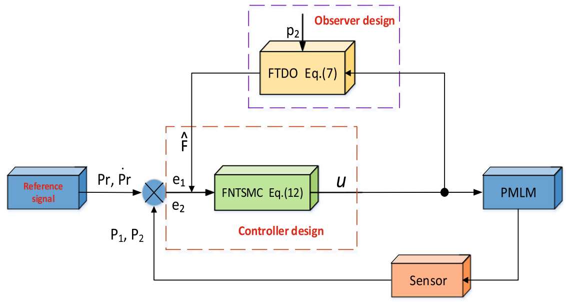

Fig. 1 The block diagram of FNTSMC based on FDTO for PMLM

4 Simulation results

In this section, simulation results are carried out to illustrate the effectiveness of the proposed control method. The simulation is accomplished in MATLAB/Simulink environment.

Let d_{load} denotes external load, F_{fric} and F_{ripple} denote friction force and ripple force, respectively. Then the lumped disturbance can be written as follows:

$$d(t) = F_{\mathrm{fric}} + F_{\mathrm{ripple}} + d_{\mathrm{load}}. \tag{46}$$

The friction force is modeled as:

$$F_{\mathrm{fric}} = [g_c + (g_s - g_c)\mathrm{e}^{-(\frac{\dot{p}_1}{g})^2} + g_v \dot{p}_1]\mathrm{sign}(\dot{p}_1), \tag{47}$$

where g_c is the Coulomb friction coefficient, g_v denotes the static friction coefficient, g_s denotes the static friction coefficient and g denotes the lubricant parameter.

The ripple force is given as:

$$F_{\mathrm{fipple}} = a_1 \sin(\omega p_1) + a_2 \sin(3\omega p_1) + a_3 \sin(5\omega p_1), \tag{48}$$

where a_1, a_2 and a_3 denote the amplitude, ω is the state-dependent ripple force frequency. The specific parameters of the PMLM system are given as $m = 5.4$ kg, $R = 16.8$ ohms, $L_f = 130$ N/A, $L_e = 123$ V/m/s, $g_c = g_v = 10$ N, $g_s = 20$ N, $g = 0.1$, $a_1 = 8.5$, $a_2 = 4.25$, $a_3 = 2.0$, $w = 314$ rad/m.

A step signal (i.e., $p_r(t) = 0.2$) and a sinusoidal signal (i.e., $p_r(t) = 0.1\sin(\frac{\pi}{2}t)$) are, respectively, viewed as the reference position. Particularly, a third-order FTDO are employed to replace n-order observer in consideration of simple structure and estimation accuracy.

The PID control algorithm and the LSMC algorithm are applied to complete the position tracking control as compare to the FNTSMC algorithm. The controllers' parameters are detailedly summarized in Tables 1 and 2.

(1) Step response

The step signal is chosen as a 0.2 m displacement. In this case, $d_{\text{load}} = 0\,\text{N}$. Under the PID, LSMC and the proposed FNTSMC, the response curves for the displacement of PMLM are shown in Fig. 2. The convergent time of PID control and LSMC approach are approximately 2 s and 1 s, respectively. Meanwhile, the convergent time of the proposed FNTSMC approach is about 0.2 s. The steady-state error range (SSER) of PID control and LSMC approach are -0.7 to 0 mm and -0.1 to 0.3 mm, respectively. Relatively, the SSER of the proposed FNTSMC approach is -0.1 to 0.1 mm. It can be concluded that the proposed FNTSMC can offer a faster convergent rate and a smaller steady-state error.

Table 1 Controllers' parameters for tracking step signal

Control schemes	Control gains
PID	$k_p = 400, k_i = 20, k_d = 6$
LSMC	$k_1 = 400, k_2 = 100, k_3 = 50,$
	$r_1 = 0.9, r_2 = 0.8, r_3 = 0.7,$
	$\beta_1 = 0.1, \beta_2 = 0.08,$
	$\gamma_1 = 1, \gamma_2 = 1, \gamma_3 = 1$
FTSMC	$k_1 = 0.005, k_2 = 400, k_3 = 100,$
	$r_1 = 0.9, r_2 = 0.8, r_3 = 0.7,$
	$\beta_1 = 0.01, \beta_2 = 0.1,$
	$\gamma_1 = 1.4, \gamma_2 = 1.5, \gamma_3 = 0.5$

Table 2 Controllers' parameters for tracking sinusoidal signal

Control Schemes	Control gains
PID	$k_p = 5000, k_i = 5000, k_d = 2000$
LSMC	$k_1 = 1500, k_2 = 1000, k_3 = 500,$
	$r_1 = 0.9, r_2 = 0.8, r_3 = 0.7,$
	$\beta_1 = 0.01, \beta_2 = 0.2,$
	$\gamma_1 = 1, \gamma_2 = 1, \gamma_3 = 1$
FTSMC	$k_1 = 400, k_2 = 200, k_3 = 200,$
	$r_1 = 0.9, r_2 = 0.8, r_3 = 0.7,$
	$\beta_1 = 0.01, \beta_2 = 0.1,$
	$\gamma_1 = 1.4, \gamma_2 = 1.5, \gamma_3 = 0.5$

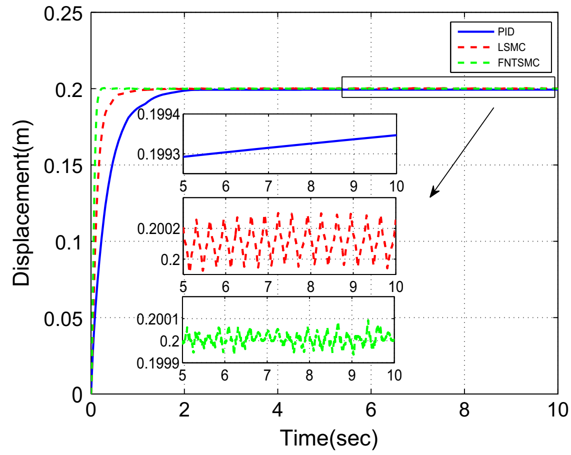

Fig. 2 The response curves for displacement under step response

(2) Tracking a sinusoid signal

A sinusoidal signal for displacement with amplitude of 0.1 m and the frequency of $\frac{\pi}{2}$ rad/s is investigated. In this case, $d_{\text{load}} = 0\text{N}$. Similarly, the response curves are given in Figs. 3 and 4. As seen from Fig. 4, the SSER of the PID control and LSMC approach are, respectively, -5 to 5 mm and -2 to 2 mm while the SSER of the FNTSMC is -0.5 to 0.5 mm. It is shown that the proposed FNTSMC can greatly reduce the steady-state error.

(3) Robustness against the load disturbance

A disturbance load with 12 N, i.e., $d_{\text{load}} = 12\,\text{N}$ is suddenly added to the control system. The correspond-

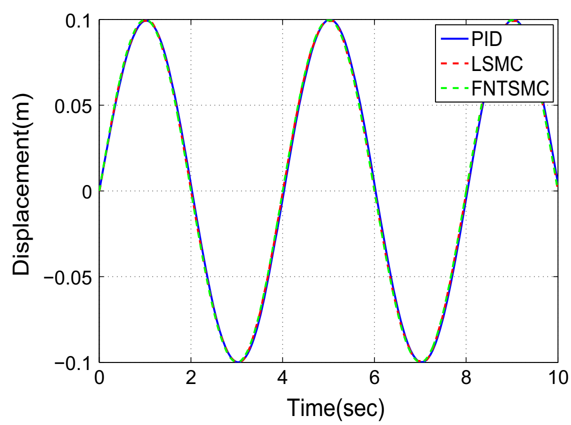

Fig. 3 The response curves of displacement for tracking a sinusoidal signal

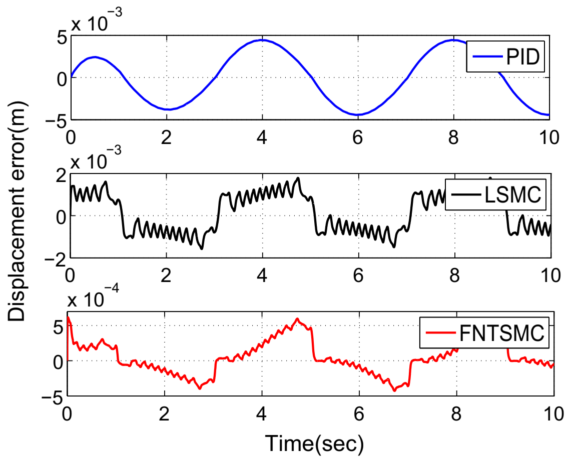

Fig. 4 The response curves of displacement error for tracking a sinusoid signal

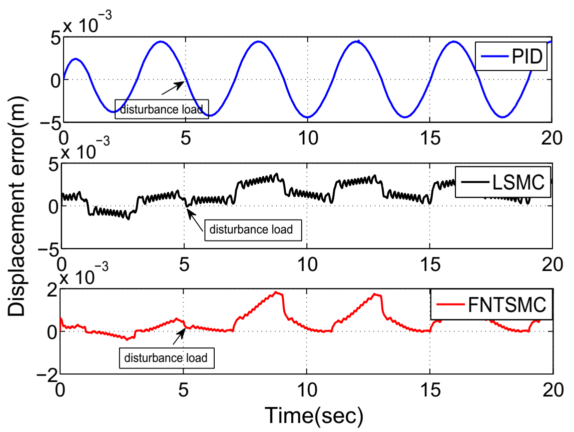

Fig. 5 The response curves for displacement error for tracking a sinusoid signal with a sudden disturbance load

ing response curves for displacement error under sinusoidal signal are shown in Fig. 5. From Fig. 5, we can see that the proposed method still possesses the smallest SSER after a sudden disturbance load at 5 s. It also indicates that the proposed approach exhibits the best robustness against the disturbance in the comparison of the three approaches.

As obviously shown in above simulation results, the proposed FNTSMC method can obtain fastest convergence rate and smallest tracking errors, i.e., can possesses preferable control property than that of the PID control method and LSMC method.

5 Conclusion

In this paper, a fast nonsingular terminal sliding mode control (FNTSMC) approach has been proposed to explore the position tracking problem of PMLM. It has been shown that the proposed control method has improved the tracking accuracy as well as restrained the chattering phenomenon. In addition, a FTDO has been applied to provide the estimation of lumped disturbance and improve robustness against the uncertainty of lumped disturbance. Simulation results have been carried out to illustrate the effectiveness of the proposed control method and correctness of theoretical analysis. Further investigation includes position tracking control of PMLM via output feedback control and the related experimental tests.

Acknowledgements This work is supported by National Natural Science Foundation of China (61673153, 61304007) and the Fundamental Research Funds for the Central Universities (JZ2017HGPA0163, JZ2016HGXJ0023).

References

1. Ji, J., Yan, S., Zhao, W., Liu, G., Zhu, X.: Minimization of cogging force in a novel linear permanent-magnet motor for artificial Hearts. IEEE Trans. Magn. **49**(7), 3901–3904 (2013)
2. Kim, J., Choi, S., Cho, K., Nam, K.: Position estimation using linear hall sensors for permanent magnet linear motor systems. IEEE Trans. Ind. Electron. **63**(12), 7644–7652 (2016)
3. Chen, S., Tan, K., Huang, S., Teo, C.: Modeling and compensation of ripples and friction in permanent-magnet linear motor using a hysteretic relay. IEEE/ASME Trans. Mechatron. **15**(4), 586–594 (2010)
4. Tan, K., Huang, S., Lee, T.: Robust adaptive numerical compensation for friction and force ripple in permanent magnet linear motors. IEEE Trans. Magn. **38**(1), 221–228 (2002)
5. Lu, Q., Zhang, X., Chen, Y., Huang, X., Ye, Y., Zhu, Z.: Modeling and investigation of thermal characteristics of a water-cooled permanent-magnet linear motor. IEEE Trans. Ind. Appl. **51**(3), 2086–2096 (2015)
6. Cao, R., Cheng, M., Zhang, B.: Speed control of complementary and modular linear flux-switching permanent-magnet motor. IEEE Trans. Ind. Electron. **62**(7), 4056–4064 (2015)
7. Utkin, V.: Sliding Modes in Control Optimization. Springer, Berlin (1992)
8. Edwards, C., Spurgeon, S.: Sliding Mode Control: Theory and Applications. Taylor and Francis, London (1998)
9. Utkin, V., Guldner, J., Shi, J.: Sliding Mode Control in Electro-mechanical Systems. CRC Press, Boca Raton (2009)

10. Cucuzzella, M., Ferrara, A.: Practical second order sliding modes in single-loop networked control of nonlinear systems. Automatica **89**, 235–240 (2018)
11. Ding, S., Li, S.: Second-order sliding mode controller design subject to mismatched term. Automatica **77**, 388–392 (2017)
12. Ding, S., Zheng, W., Sun, J., Wang, J.: Second-order sliding mode controller design and its implementation for buck converters. IEEE Trans. Ind. Inform. **14**(5), 1990–2000 (2018)
13. Qi, W., Zong, G., Karimi, H.R.: Observer-based adaptive SMC for nonlinear uncertain singular semi-Markov jump systems with applications to DC motor. IEEE Trans. Circuits Syst. I Regul. Pap. **65**(9), 2951–2960 (2018)
14. Weng, Y., Gao, X.: Adaptive sliding mode decoupling control with data-driven sliding surface for unknown MIMO nonlinear discrete systems. Circuits Syst. Signal Process. **36**(3), 969–997 (2017)
15. Weng, Y., Gao, X.: Data-driven robust output tracking control for gas collector pressure system of coke ovens. IEEE Trans. Ind. Electron. **64**(5), 4187–4198 (2017)
16. Du, H., Zhai, J., Chen, M., Zhu, W.: Robustness analysis of a continuous higher-order finite-time control system under sampled-data control. IEEE Trans. Autom. Control **64**(6), 2488–2494 (2019)
17. Du, H., Jiang, C., Wen, G., Zhu, W., Cheng, Y.: Current sharing control for parallel DC–DC buck converters based on finite-time control technique. IEEE Trans. Ind. Inform. **15**(4), 2186–2198 (2019)
18. Shen, H., Li, F., Yan, H., Karimi, H.R., Lam, H.K.: Finite-time event-triggered Hontrol for T–S fuzzy Markov jump systems. IEEE Trans. Fuzzy Syst. **26**(5), 3122–3135 (2018)
19. Jin, M., Lee, J., Chang, P., Choi, C.: Practical nonsingular terminal sliding-mode control of robot manipulators for high-accuracy tracking control. IEEE Trans. Ind. Electron. **56**(9), 3593–3601 (2009)
20. Man, Z., Paplinski, A., Wu, H.: A robust MIMO terminal sliding mode control scheme for rigid robotic manipulators. IEEE Trans. Autom. Control **39**(12), 2464–2469 (1994)
21. Cheng, J., Park, J.H., Karimi, H.R., Shen, H.: A flexible terminal approach to sampled-data exponentially synchronization of Markovian neural networks with time-varying delayed signals. IEEE Trans. Cybern. **48**(8), 2232–2244 (2018)
22. Li, S., Zhou, M., Yu, X.: Design and implementation of terminal sliding mode control method for PMSM speed regulation system. IEEE Trans. Ind. Inform. **9**(4), 1879–1891 (2013)
23. Feng, Y., Yu, X., Man, Z.: Non-singular terminal sliding mode control of rigid manipulators. Automatica **38**(12), 2159–2167 (2002)
24. Sun, G., Ma, Z.: Practical tracking control of linear motor with adaptive fractional order terminal sliding mode control. IEEE/ASME Trans. Mechatron. **22**(6), 2643–2653 (2017)
25. Sun, G., Wu, L., Man, Z., Ma, Z., Liu, J.: Practical tracking control of linear motor via fractional-order sliding mode. Automatica **94**, 221–235 (2018)
26. Sun, G., Ma, Z., Yu, J.: Discrete-time fractional order terminal sliding mode tracking control for linear motor. IEEE Trans. Ind. Electron. **65**(4), 3386–3394 (2018)
27. Feng, Y., Han, F., Yu, X.: Chattering free full-order sliding-mode control. Automatica **50**(4), 1310–1314 (2014)
28. Yu, X., Man, Z.: Fast terminal sliding-mode control design for nonlinear dynamical systems. IEEE Trans. Circuits Syst. I Fundam. Theory Appl. **49**(2), 261–264 (2002)
29. Zheng, J., Wang, H., Man, Z., Jin, J., Fu, M.: Robust motion control of a linear motor positioner using fast nonsingular terminal sliding mode. IEEE/ASME Trans. Mechatron. **20**(4), 1743–1752 (2015)
30. Du, H., Chen, X., Wen, G., Yu, X., Lu, J.: Discrete-time fast terminal sliding mode control for permanent magnet linear motor. IEEE Trans. Ind. Electron. **65**(12), 9916–9927 (2018)
31. Mo, X., Lan, Q.: Finite-time integral sliding mode control for motion control of permanent-magnet linear motors. Math. Probl. Eng. **4**, 389–405 (2013)
32. Zhang, L., Wei, C., Jing, L., Cui, N.: Fixed-time sliding mode attitude tracking control for a submarine-launched missile with multiple disturbances. Nonlinear Dyn. **93**(4), 2543–2563 (2018)
33. Zhang, B., Jia, Y.: Fixed-time consensus protocols for multi-agent systems with linear and nonlinear state measurements. Nonlinear Dyn. **82**(4), 1683–1690 (2015)
34. Shen, H., Li, F., Yan, H., Karimi, H.R., Lam, H.K.: Finite-time event-triggered Hontrol for T–S fuzzy Markov jump systems. Nonlinear Dyn. **82**(4), 1683–1690 (2015)
35. Wu, D., Du, H., Wen, G., Lu, J.: Fixed-time synchronization control for a class of master-slave systems based on homogeneous method. IEEE Trans. Circuits Syst. II Express Briefs (2018). https://doi.org/10.1109/TCSII.2018.2886574
36. Chen, W., Yang, J., Guo, L., Li, S.: Disturbance-observer-based control and related methods—an overview. IEEE Trans. Ind. Electron. **63**(2), 1083–1095 (2016)
37. Liu, S., Liu, Y., Wang, N.: Nonlinear disturbance observer-based backstepping finite-time sliding mode tracking control of underwater vehicles with system uncertainties and external disturbances. Nonlinear Dyn. **88**(1), 465–476 (2017)
38. Sun, H., Li, S., Sun, C.: Finite time integral sliding mode control of hypersonic vehicles. Nonlinear Dyn. **73**(1–2), 229–244 (2013)
39. Aurora, C., Ferrara, A.: A sliding mode observer for sensorless induction motor speed regulation. Int. J. Syst. Sci. **38**(11), 913–929 (2007)
40. Rinaldi, G., Menon, P., Edwards, C., Ferrara, A.: Sliding mode based dynamic state estimation for synchronous generators in power systems. IEEE Control Syst. Lett. **2**(4), 785–790 (2018)
41. Du, H., Qian, C., Yang, S., Li, S.: Recursive design of finite-time convergent observers for a class of time-varying nonlinear systems. Automatica **49**(2), 601–609 (2013)
42. Lin, X., Li, S., Zou, Y.: Finite-time stabilization of switched linear time-delay systems with saturating actuators. Appl. Math. Comput. **299**, 66–79 (2017)
43. Ahn, H., Chen, Y., Dou, Y.: State-periodic adaptive compensation of cogging and coulomb friction in permanent-magnet linear motors. IEEE Trans. Magn. **41**(1), 90–98 (2005)
44. Bhat, S.P., Bernstein, D.S.: Finite-time stability of continuous autonomous systems. SIAM J. Control Optim. **38**(3), 751–766 (2000)
45. Polyakov, A.: Nonlinear feedback design for fixed-time stabilization of linear control systems. IEEE Trans. Autom. Control **57**(8), 2106–2110 (2012)
46. Hardy, G., Littlewood, J., Polya, G.: Inequalities. Cambridge University Press, Cambridge (1952)

47. Qian, C., Lin, W.: A continuous feedback approach to global strong stabilization of nonlinear systems. IEEE Trans. Autom. Control **46**(7), 1061–1079 (2001)